Mathematical Biosciences 375 (2024) 109258

Contents lists available at ScienceDirect

Mathematical Biosciences

journal homepage: www.elsevier.com/locate/mbs

Original Research Article

Infection thresholds for two interacting pathogens in a wild animal population

M.G. Roberts

New Zealand Institute for Advanced Study and the Infectious Disease Research Centre, Massey University, Private Bag 102 904, North Shore Mail Centre, Auckland, New Zealand

ARTICLE INFO

Keywords:
Ecology
Epidemiology
Basic reproduction number
Next-generation matrix
Interacting pathogen variants
Invasion thresholds

ABSTRACT

We present a model for the dynamics of two interacting pathogen variants in a wild animal host population. Using the next-generation matrix approach we define the invasion threshold for one pathogen variant when the other is already established and at steady state. We then provide explicit criteria for the special cases where: i) the two pathogen variants exclude each other; ii) one variant excludes the other; iii) the population dynamics of hosts infected with both variants are independent of the order of infection; iv) there is no interaction between the variants; and v) one variant enhances transmission of the other.

1. Introduction

The use of mathematical models to describe the dynamics of infectious diseases is now well established [1,2]. Mathematical investigations of the dynamics of co-infections have found a variety of behaviours. For example, Gao et al. [3] analysed the dynamics of two diseases in a single host population. They employed an *SIS* model with no increased mortality due to infection, and noticed the potential for dynamics including backward bifurcation, bistability and Hopf bifurcation. The majority of research into co-infection dynamics has been motivated by the interactions between infectious diseases of humans. Examples include the interactions between HIV and tuberculosis [4,5], syphilis [6] and malaria [7]. These studies address the problem of another infection enhancing the progression of the infection with HIV, and of HIV accelerating the infection with the other pathogen. There is currently interest in the interaction of Covid-19 with other pathogens (e.g. [8]). Studies of interacting pathogens in ecosystems are less common (see [9] p.286). These have addressed parasite communities (e.g. [10]) and vector-borne diseases (e.g. [11, 12]) among applications, and the potential for Wolbachia infection to control mosquitos and hence malaria (e.g. [13]). When more than two pathogens are involved the dimension of the system may become problematic, requiring a strategy for model reduction [14].

In the present paper we model the dynamics of a single host species and two pathogen variants. The variants could be different species of pathogen or different strains of the same pathogen. We take the host to be a wild animal with density-dependent birth and death rates, no recovery from infection and increased mortality due to infection. We focus on finding the threshold quantity that determines if one of the pathogen variants can invade a host population that is already infected and at steady state with the other variant. We explicitly address special cases where: (i) the two variants exclude each other; (ii) one variant excludes the other; (iii) the population dynamics of hosts infected with both variants are independent of the order of infection; (iv) there is no interaction between the variants; and (v) infection with one pathogen variant enhances the transmission of the other variant.

2. The model

Let N be the density of the host population, and I_1 and I_2 be the population densities of hosts infected with pathogen variants one and two respectively. Let I_3 be the density of hosts infected with pathogen variant one (PV1) and then pathogen variant two (PV2), and I_4 be the density of hosts infected with PV2 and then PV1. Hence the density of hosts infected with both variants is $I_3 + I_4$. The dynamics of the host population can be modelled by the differential equation

$$\frac{\mathrm{d}N}{\mathrm{d}t} = \{\nu(N) - \mu(N)\}\, N - \sum_{j=1}^{4} \alpha_j I_j \tag{1}$$

Host birth and death rates, ν and μ respectively, may be density-dependent, with $\nu'(N) \leqslant 0$ and $\mu'(N) \geqslant 0$, with $\nu'(N) \neq \mu'(N)$ for all $N > 0$. The α_j represent the increased mortality rate due to infection. The steady state infection-free carrying capacity is $N = K$, where $\nu(K) = \mu(K)$ and $I_j = 0$ for $j = 1, 2, 3, 4$. The dynamics of the sub-populations of hosts infected with a single pathogen variant are

E-mail address: m.g.roberts@massey.ac.nz.

https://doi.org/10.1016/j.mbs.2024.109258
Received 5 July 2023; Received in revised form 5 July 2024; Accepted 8 July 2024
Available online 14 July 2024

modelled by

$$\frac{\mathrm{d}I_1}{\mathrm{d}t} = \lambda_1 S - \left\{\mu(N) + \alpha_1 + \lambda_3\right\} I_1 \qquad (2)$$
$$\frac{\mathrm{d}I_2}{\mathrm{d}t} = \lambda_2 S - \left\{\mu(N) + \alpha_2 + \lambda_4\right\} I_2$$

where $S = N - \sum_{j=1}^{4} I_j$ is the population density of susceptible hosts, λ_1 and λ_2 are the infection pressures of PV1 and PV2 respectively on susceptible hosts, λ_3 is the infection pressure of PV2 on hosts already infected with PV1, and λ_4 is the infection pressure of PV1 on hosts already infected with PV2. Assuming mass action, the λ_j may be represented by

$$\begin{pmatrix}\lambda_1\\ \lambda_2\\ \lambda_3\\ \lambda_4\end{pmatrix} = \begin{pmatrix}\beta_{11} & 0 & \beta_{13} & \beta_{14}\\ 0 & \beta_{22} & \beta_{23} & \beta_{24}\\ 0 & \beta_{32} & \beta_{33} & \beta_{34}\\ \beta_{41} & 0 & \beta_{43} & \beta_{44}\end{pmatrix}\begin{pmatrix}I_1\\ I_2\\ I_3\\ I_4\end{pmatrix} \qquad (3)$$

where the β_{ij} are constants for all subscripts i and j. The dynamics of the sub-populations of hosts infected with both pathogen variants are modelled by

$$\frac{\mathrm{d}I_3}{\mathrm{d}t} = \lambda_3 I_1 - \left\{\mu(N) + \alpha_3\right\} I_3 \qquad (4)$$
$$\frac{\mathrm{d}I_4}{\mathrm{d}t} = \lambda_4 I_2 - \left\{\mu(N) + \alpha_4\right\} I_4$$

The system modelled by Eqs. (1)–(4) has four steady states.

1. The infection-free steady state: $N = K$, $I_j = 0$ for $j = 1, 2, 3, 4$, is stable if
$$\mathcal{R}^{\#} = \frac{\beta_{11}K}{\mu(K) + \alpha_1} < 1 \quad \text{and} \quad \mathcal{R}^{\flat} = \frac{\beta_{22}K}{\mu(K) + \alpha_2} < 1$$
2. The steady state with PV1 only: $N = N^{\#}$, $I_1 = I_1^{\#}$, with $I_2 = I_3 = I_4 = 0$, exists if $\mathcal{R}^{\#} > 1$. The host population density is bounded, $\alpha_1/\beta_{11} < N^{\#} < K$.
3. The steady state with PV2 only: $N = N^{\flat}$, $I_2 = I_2^{\flat}$, with $I_1 = I_3 = I_4 = 0$, exists if $\mathcal{R}^{\flat} > 1$. The host population density is bounded, $\alpha_2/\beta_{22} < N^{\flat} < K$.
4. The steady state with both variants present: $N = N^{\star}$, $I_j = I_j^{\star}$ for $j = 1, 2, 3, 4$. Conditions for the existence of this steady state are addressed below. As $I_j^{\star} > 0$ for $j = 1, 2$ and $I_j^{\star} \geqslant 0$ for $j = 3, 4$, Eq. (1) ensures that $N^{\star} < K$.

Details of the calculation of the steady states with a single pathogen variant are presented in Appendix A. In Appendix B we derive the Jacobian stability matrix, and discuss how it may be used to derive the next-generation matrix (NGM), and hence determine the stability of the steady states with a single pathogen variant present. Here we summarise the stability results for the steady states with a single pathogen variant present, finding criteria for invasion by the alternative pathogen. We discuss five special cases: (i) PV1 and PV2 exclude each other in a host; (ii) either PV2 excludes PV1 or PV1 excludes PV2; (iii) the order of infection with PV1 and PV2 does not influence the dynamics of host populations infected with both pathogens; (iv) the situation where the two pathogens do not interact; and (v) either infection with PV2 enhances susceptibility to PV1 or infection with PV1 enhances susceptibility to PV2.

2.1. Steady states with a single pathogen variant

The steady state with PV1 only present: $N = N^{\#}$, $I = I_1^{\#}$ with $I_2 = I_3 = I_4 = 0$, exists if $\mathcal{R}^{\#} > 1$. The steady state is unstable and PV2 can invade the host population if $\mathcal{Q}^{\#} = \rho(\mathbf{K}^{\#}) > 1$, where $\mathbf{K}^{\#}$ is the NGM for PV2 with PV1 present ($\mathcal{Q}^{\#}$ is the largest eigenvalue of the matrix $\mathbf{K}^{\#}$).

$$\mathbf{K}^{\#} = \begin{pmatrix}\beta_{22}T_2^{\#}S^{\#} + \beta_{41}I_1^{\#}T_2^{\#}\beta_{24}T_4^{\#}S^{\#} & \beta_{23}T_3^{\#}S^{\#}\\ \beta_{32}T_2^{\#}I_1^{\#} + \beta_{41}I_1^{\#}T_2^{\#}\beta_{34}T_4^{\#}I_1^{\#} & \beta_{33}T_3^{\#}I_1^{\#}\end{pmatrix} \qquad (5)$$

where $S^{\#} = N^{\#} - I_1^{\#}$ is the proportion of hosts susceptible to infection with either pathogen. Following invasion of this steady state by PV2, the expected times spent infectious with PV2 in compartments I_2, I_3 and I_4 respectively are

$$T_2^{\#} = \frac{1}{\mu(N^{\#}) + \alpha_2 + \beta_{41}I_1^{\#}} \qquad T_3^{\#} = \frac{1}{\mu(N^{\#}) + \alpha_3} \qquad T_4^{\#} = \frac{1}{\mu(N^{\#}) + \alpha_4}$$

The evaluation of the NGM via the Jacobian matrix is presented in Appendix B. The NGM can also be constructed as follows. At the steady state there are $S^{\#}$ uninfected hosts and $I_1^{\#}$ hosts infected with PV1 only. Hosts infected with PV2 only infect these hosts at rates $\beta_{22}I_2$ and $\beta_{32}I_2$ respectively, and stay infectious for expected time $T_2^{\#}$. Hosts infected with PV1 and subsequently with PV2 infect the two host sub-populations at rates $\beta_{23}I_3$ and $\beta_{33}I_3$ respectively, and stay infectious for expected time $T_3^{\#}$. A proportion $\beta_{41}I_1^{\#}T_2^{\#}$ of hosts infected with PV2 are subsequently infected with PV1, then infect the two host sub-populations at rates $\beta_{24}I_4$ and $\beta_{34}I_4$ respectively, and stay infectious for expected time $T_4^{\#}$. An illustration of these transitions is shown in Fig. 1A.

Define the quantities $\mathcal{Q}_2 = \beta_{22}T_2^{\#}S^{\#}$, $\mathcal{Q}_3^{\#} = \beta_{33}T_3^{\#}I_1^{\#}$ and $\mathcal{Q}_4^{\#} = \beta_{44}T_4^{\#}I_1^{\#}$. The characteristic polynomial of $\mathbf{K}^{\#}$ is

$$X^{\#}(x) = x^2 - \left(\mathcal{Q}_2 + \mathcal{Q}_3^{\#} + k_2\mathcal{Q}_2\mathcal{Q}_4^{\#}\right)x - \left(k_1 - 1\right)\mathcal{Q}_2\mathcal{Q}_3^{\#} - k_2\left(k_3 - 1\right)\mathcal{Q}_2\mathcal{Q}_3^{\#}\mathcal{Q}_4^{\#}$$

where $k_1 = \dfrac{\beta_{23}\beta_{32}}{\beta_{22}\beta_{33}}$, $k_2 = \dfrac{\beta_{24}\beta_{41}}{\beta_{22}\beta_{44}}$ and $k_3 = \dfrac{\beta_{23}\beta_{34}}{\beta_{24}\beta_{33}}$. Hence

$$\mathcal{Q}^{\#} = \frac{\mathcal{Q}_2 + \mathcal{Q}_3^{\#} + k_2\mathcal{Q}_2\mathcal{Q}_4^{\#}}{2} \times \left(1 + \sqrt{1 + \frac{4\left(k_1 - 1\right)\mathcal{Q}_2\mathcal{Q}_3^{\#} + 4k_2\left(k_3 - 1\right)\mathcal{Q}_2\mathcal{Q}_3^{\#}\mathcal{Q}_4^{\#}}{\left(\mathcal{Q}_2 + \mathcal{Q}_3^{\#} + k_2\mathcal{Q}_2\mathcal{Q}_4^{\#}\right)^2}}\right) \qquad (6)$$

Similarly, the steady state with PV2 only present, $N = N^{\flat}$, $I_2 = I_2^{\flat}$ with $I_1 = I_3 = I_4 = 0$, exists when $\mathcal{R}^{\flat} > 1$. Pathogen variant one can invade this steady state if $\mathcal{Q}^{\flat} = \rho(\mathbf{K}^{\flat}) > 1$, where

$$\mathbf{K}^{\flat} = \begin{pmatrix}\beta_{11}T_1^{\flat}S^{\flat} + \beta_{32}I_2^{\flat}T_1^{\flat}\beta_{13}T_3^{\flat}S^{\flat} & \beta_{14}T_4^{\flat}S^{\flat}\\ \beta_{41}T_1^{\flat}I_2^{\flat} + \beta_{32}I_2^{\flat}T_1^{\flat}\beta_{43}T_3^{\flat}I_2^{\flat} & \beta_{44}T_4^{\flat}I_2^{\flat}\end{pmatrix} \qquad (7)$$

$S^{\flat} = N^{\flat} - I_1^{\flat}$ is the proportion of hosts susceptible to infection with either pathogen; and the expected times spent infectious with PV1 in compartments I_1, I_3 and I_4 respectively are

$$T_1^{\flat} = \frac{1}{\mu(N^{\flat}) + \alpha_1 + \beta_{32}I_2^{\flat}} \qquad T_3^{\flat} = \frac{1}{\mu(N^{\flat}) + \alpha_3} \qquad T_4^{\flat} = \frac{1}{\mu(N^{\flat}) + \alpha_4}$$

The transitions involved in the construction of $\mathbf{K}^{\flat}$ are illustrated in Fig. 1B.

Define the quantities $\mathcal{Q}_1 = \beta_{11}T_1^{\flat}S^{\flat}$, $\mathcal{Q}_3^{\flat} = \beta_{33}T_3^{\flat}I_2^{\flat}$ and $\mathcal{Q}_4^{\flat} = \beta_{44}T_4^{\flat}I_2^{\flat}$. The characteristic polynomial of $\mathbf{K}^{\flat}$ is

$$X^{\flat}(x) = x^2 - \left(\mathcal{Q}_1 + \ell_2\mathcal{Q}_1\mathcal{Q}_3^{\flat} + \mathcal{Q}_4^{\flat}\right)x - \left(\ell_1 - 1\right)\mathcal{Q}_1\mathcal{Q}_4^{\flat} - \ell_2\left(\ell_3 - 1\right)\mathcal{Q}_1\mathcal{Q}_3^{\flat}\mathcal{Q}_4^{\flat}$$

where $\ell_1 = \dfrac{\beta_{14}\beta_{41}}{\beta_{11}\beta_{44}}$, $\ell_2 = \dfrac{\beta_{13}\beta_{32}}{\beta_{11}\beta_{33}}$ and $\ell_3 = \dfrac{\beta_{14}\beta_{43}}{\beta_{13}\beta_{44}}$. Hence

$$\mathcal{Q}^{\flat} = \frac{\mathcal{Q}_1 + \ell_2\mathcal{Q}_1\mathcal{Q}_3^{\flat} + \mathcal{Q}_4^{\flat}}{2} \times \left(1 + \sqrt{1 + \frac{4\left(\ell_1 - 1\right)\mathcal{Q}_1\mathcal{Q}_4^{\flat} + 4\ell_2\left(\ell_3 - 1\right)\mathcal{Q}_1\mathcal{Q}_3^{\flat}\mathcal{Q}_4^{\flat}}{\left(\mathcal{Q}_1 + \ell_2\mathcal{Q}_1\mathcal{Q}_3^{\flat} + \mathcal{Q}_4^{\flat}\right)^2}}\right) \qquad (8)$$

We now explore some special cases of the interactions between the two pathogen variants. For Special Cases 1–4, $k_3 = \ell_3 = 1$, for Special Case 5 we choose values of the β_{ij} that also obey these equalities, although they may not hold in general. Bifurcation diagrams with the steady state solutions found numerically are presented in Figs. 2–4. In deriving the figures $\mathcal{R}^{\flat} = 1.9$ was held constant, and steady states were found in the range $0.8 < \mathcal{R}^{\#} < 2.5$ (Figs. 2, 3) or $0.3 < \mathcal{R}^{\#} < 2.0$ (Fig. 4). In

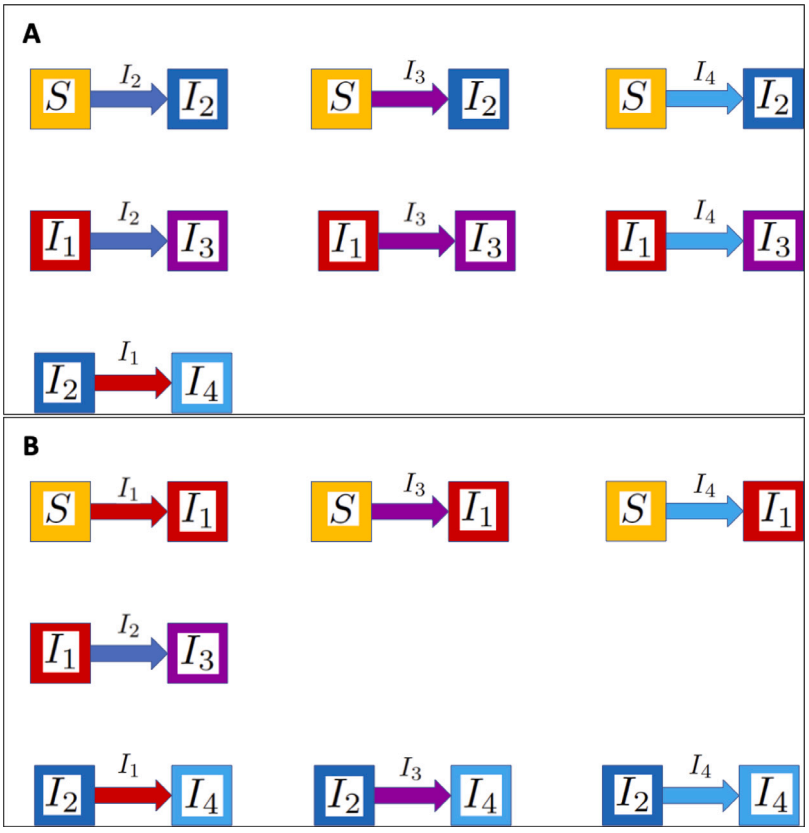

Fig. 1. Transmission routes for the invasion of a host population infected with one pathogen variant by a second variant. A: A population infected with pathogen variant one (PV1) invaded by pathogen variant two (PV2). B: A population infected with PV2 invaded by PV1. S: susceptible host population; I_1: infected with PV1 only; I_2: infected with PV2 only; I_3: infected with PV1 and subsequently infected with PV2; I_4: infected with PV2 and subsequently infected with PV1. Each state variable is represented by a square. Labelled arrows of the same colour indicate the infected host type responsible for transition between states.

all figures the value of $\mathcal{R}^{\#}$ was increased by reducing α_1 with all other parameters held constant. The parameter values used for the examples are summarised in Table 1.

2.2. Special cases

Special Case 1. Two pathogen variants with no coinfection.

If infection with one of the pathogen variants prevents infection with the other variant, then $I_3 = I_4 = 0$. We then have $\lambda_1 = \beta_{11} I_1$, $\lambda_2 = \beta_{22} I_2$, $\lambda_3 = \lambda_4 = 0$ and $\mathcal{Q}_3^{\#} = \mathcal{Q}_4^{\#} = \mathcal{Q}_3^{\flat} = \mathcal{Q}_4^{\flat} = 0$. Hence, from Eqs. (6), (8)

$$\mathcal{Q}^{\#} = \mathcal{Q}_2 = \frac{\beta_{22}\left(N^{\#} - I_1^{\#}\right)}{\mu(N^{\#}) + \alpha_2} \qquad \mathcal{Q}^{\flat} = \mathcal{Q}_1 = \frac{\beta_{11}\left(N^{\flat} - I_2^{\flat}\right)}{\mu(N^{\flat}) + \alpha_1}$$

The steady state $\left(N^{\#}, I_1^{\#}, 0\right)$ is stable if $\mathcal{Q}_2 < 1$ and the steady state $\left(N^{\flat}, 0, I_2^{\flat}\right)$ is stable if $\mathcal{Q}_1 < 1$. Setting the right-hand sides of Eqs. (2) to zero, we find that at a steady state with both variants present the host population density solves

$$\mu(N) = \frac{\alpha_1\beta_{22} - \alpha_2\beta_{11}}{\beta_{11} - \beta_{22}} \tag{9}$$

Given the solution $N = N^{\star}$ of Eq. (9), we derive

$$I_1^{\star} = \frac{\nu(N^{\star})N^{\star}}{\alpha_1 - \alpha_2} - \frac{\beta_{22}N^{\star} - \alpha_2}{\beta_{11} - \beta_{22}} \qquad I_2^{\star} = \frac{\beta_{11}N^{\star} - \alpha_1}{\beta_{11} - \beta_{22}} - \frac{\nu(N^{\star})N^{\star}}{\alpha_1 - \alpha_2}$$

If (without loss of generality) $\beta_{11} > \beta_{22}$, then $\mu(N^{\star}) > 0$ implies $\alpha_1 > \alpha_2$. A bifurcation diagram illustrating the dynamics is presented in Fig. 2. The figure shows that as $\mathcal{R}^{\#}$ is increased the stable steady state changes from one with PV2 only present to the state with both variants present when $\mathcal{Q}^{\flat} = 1$. There is a second bifurcation to the state with PV1 only present at $\mathcal{Q}^{\#} = 1$.

Special Case 2. One pathogen variant excludes the other variant.

If being infected with PV2 excludes infection with PV1, then we always have $I_4 = 0$. The NGM for PV2 at the steady state $\left(N^{\#}, I_1^{\#}, 0\right)$ is

$$\mathbf{K}^{\#} = \begin{pmatrix} \dfrac{\beta_{22}\left(N^{\#} - I_1^{\#}\right)}{\mu(N^{\#}) + \alpha_2} & \dfrac{\beta_{23}\left(N^{\#} - I_1^{\#}\right)}{\mu(N^{\#}) + \alpha_3} \\ \dfrac{\beta_{32} I_1^{\#}}{\mu(N^{\#}) + \alpha_2} & \dfrac{\beta_{33} I_1^{\#}}{\mu(N^{\#}) + \alpha_3} \end{pmatrix}$$

with spectral radius

$$\mathcal{Q}^{\#} = \frac{\mathcal{Q}_2 + \mathcal{Q}_3^{\#}}{2}\left(1 + \sqrt{1 + \frac{4\left(k_1 - 1\right)\mathcal{Q}_2\mathcal{Q}_3^{\#}}{\left(\mathcal{Q}_2 + \mathcal{Q}_3^{\#}\right)^2}}\right)$$

As PV2 excludes PV1, $\mathcal{Q}_4^{\flat} = 0$ and $\mathcal{Q}^{\flat} = \mathcal{Q}_1 + \ell_2\mathcal{Q}_1\mathcal{Q}_3^{\flat}$. For the example illustrated in Fig. 3A we took $\lambda_1 = \beta_{11}\left(I_1 + I_3\right)$, $\lambda_2 = \lambda_3 = \beta_{22}\left(I_2 + I_3\right)$, $\lambda_4 = 0$, and $\alpha_3 = \alpha_1 + \alpha_2$. Fig. 3A shows that as $\mathcal{R}^{\#}$ is increased, the stable steady state changes from one with PV2 only present to the state with both variants present. The bifurcation occurs when $\mathcal{Q}^{\flat} = 1$.

Similarly, if being infected with PV1 excludes infection with PV2 we have $I_3 = 0$, $\mathcal{Q}^{\#} = \mathcal{Q}_2 + k_2\mathcal{Q}_2\mathcal{Q}_4^{\#}$ and

$$\mathcal{Q}^{\flat} = \frac{\mathcal{Q}_1 + \mathcal{Q}_4^{\flat}}{2}\left(1 + \sqrt{1 + \frac{4\left(\ell_1 - 1\right)\mathcal{Q}_1\mathcal{Q}_4^{\flat}}{\left(\mathcal{Q}_1 + \mathcal{Q}_4^{\flat}\right)^2}}\right)$$

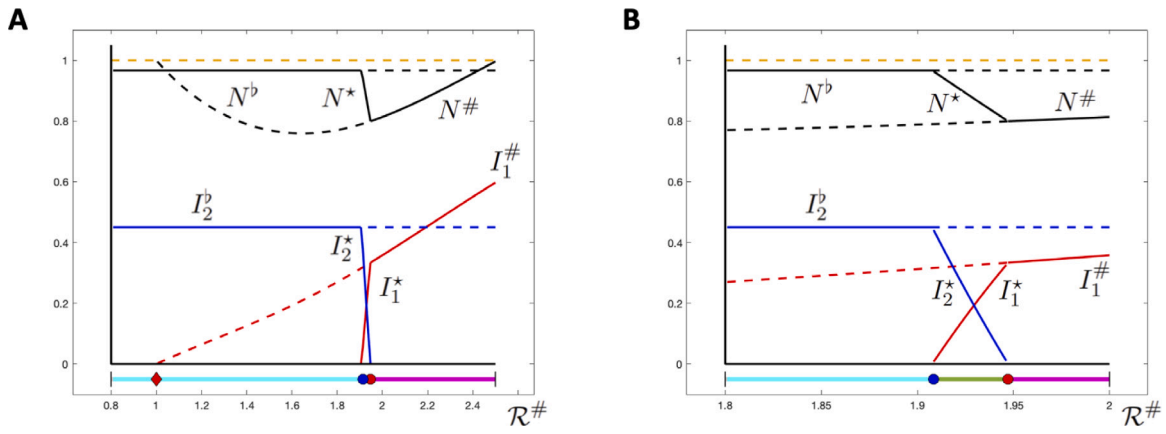

Fig. 2. A: Bifurcation diagram against $\mathcal{R}^\#$ for Special Case 1 where infection with one pathogen variant excludes the other. Host population density shown in black, density of hosts infected with pathogen variant one and pathogen variant two in red and blue respectively, host carrying capacity in orange. Solid curves show a stable steady state, broken curves an unstable state. The lower bars indicate the stable steady state at that value of $\mathcal{R}^\#$. Magenta: $(N^\#, I_1^\#, 0)$; Cyan: $(N^\flat, 0, I_2^\flat)$; Green: $(N^\star, I_1^\star, I_2^\star)$. At the red diamond $\mathcal{R}^\# = 1$, at the blue circle $\mathcal{Q}^\flat = 1$, at the red circle $\mathcal{Q}^\# = 1$. B: The diagram expanded in the range $1.8 < \mathcal{R}^\# < 2.0$.

Table 1
Parameter values used in the examples.

Birth rate of hosts	$\nu = 1.0\,\text{yr.}^{-1}$ constant.
Minimum death rate of hosts	$\mu(0) = 0.4\,\text{yr.}^{-1}$.
Host carrying capacity	$K = 1.0$ bm..
Pathogen reproduction numbers	
Special Cases 1–4	$0.8 \leqslant \mathcal{R}^\# \leqslant 2.5$; $\mathcal{R}^\flat = 1.9$.
Special Case 5	$0.3 \leqslant \mathcal{R}^\# \leqslant 2.0$; $\mathcal{R}^\flat = 1.9$.
Pathogen-induced mortality	$0.0036 \leqslant \alpha_1 \leqslant 2.1364\,\text{yr.}^{-1}$; $\alpha_2 = 0.0431\,\text{yr.}^{-1}$.
Special Case 1	$\alpha_3 = \alpha_4 = 0$.
Special Case 2 Example 1	$\alpha_3 = \alpha_1 + \alpha_2$; $\alpha_4 = 0$.
Special Case 2 Example 2	$\alpha_3 = 0$; $\alpha_4 = \alpha_1 + \alpha_2$.
Special Case 3	$\alpha_3 = \alpha_4 = \alpha_1 + \alpha_2$.
Special Case 4	$\alpha_3 = \alpha_4 = \max(\alpha_1, \alpha_2)$.
Special Case 5	$\alpha_3 = \alpha_4 = \alpha_1 + \alpha_2$.
Transmission coefficients	
Pathogen variant one	$\beta_{11} = 2.5091\,\text{bm.}^{-1}\,\text{yr.}^{-1}$.
Pathogen variant two	$\beta_{22} = 1.9818\,\text{bm.}^{-1}\,\text{yr.}^{-1}$.
Special Case 1	$\beta_{ij} = 0$ unless $i = j = 1$ or $i = j = 2$.
Special Case 2 Example 1	$\beta_{13} = \beta_{11}$; $\beta_{23} = \beta_{32} = \beta_{33} = \beta_{22}$; $\beta_{ij} = 0$ otherwise.
Special Case 2 Example 2	$\beta_{14} = \beta_{41} = \beta_{44} = \beta_{11}$; $\beta_{24} = \beta_{22}$; $\beta_{ij} = 0$ otherwise.
Special Case 3	$\beta_{41} = \beta_{11}$; $\beta_{13} = \beta_{14} = \beta_{43} = \beta_{44} = \beta_{11}/2$; $\beta_{32} = \beta_{22}$; $\beta_{23} = \beta_{24} = \beta_{33} = \beta_{34} = \beta_{22}/2$.
Special Case 4	$\beta_{13} = \beta_{14} = \beta_{41} = \beta_{43} = \beta_{44} = \beta_{11}$; $\beta_{23} = \beta_{24} = \beta_{32} = \beta_{33} = \beta_{34} = \beta_{22}$.
Special Case 5 Example 1	$\beta_{13} = \beta_{14} = \beta_{11}$; $\beta_{41} = \beta_{43} = \beta_{44} = 3\beta_{11}/2$; $\beta_{23} = \beta_{24} = \beta_{32} = \beta_{33} = \beta_{34} = \beta_{22}$.
Special Case 5 Example 2	$\beta_{13} = \beta_{14} = \beta_{41} = \beta_{43} = \beta_{44} = \beta_{11}$; $\beta_{23} = \beta_{24} = \beta_{22}$; $\beta_{32} = \beta_{33} = \beta_{34} = 3\beta_{22}/2$.

bm. signifies one unit of biomass per unit area.

This example is illustrated in Fig. 3B with $\lambda_1 = \lambda_4 = \beta_{11}(I_1 + I_4)$, $\lambda_2 = \beta_{22}(I_2 + I_4)$, $\lambda_3 = 0$, and $\alpha_4 = \alpha_1 + \alpha_2$. Fig. 3B shows that as $\mathcal{R}^\#$ is increased, the stable steady state changes from one with PV2 only present to the state with both variants present at $\mathcal{Q}^\flat = 1$, with a second bifurcation to the state with PV1 only present at $\mathcal{Q}^\# = 1$.

Special Case 3. Order of infection immaterial.

If a host infected concurrently with both pathogen variants reacts in the same way, regardless of whether PV1 or PV2 infected first, then $\mathcal{Q}_3^\# = \mathcal{Q}_4^\#$, $\mathcal{Q}_3^\flat = \mathcal{Q}_4^\flat$, $k_3 = \ell_3 = 1$, and $\alpha_4 = \alpha_3$. Hence

$$\mathcal{Q}^\# = \frac{\mathcal{Q}_2 + \mathcal{Q}_3^\# + k_2\mathcal{Q}_2\mathcal{Q}_3^\#}{2}\left(1 + \sqrt{1 + \frac{4(k_1 - 1)\mathcal{Q}_2\mathcal{Q}_3^\#}{\left(\mathcal{Q}_2 + \mathcal{Q}_3^\# + k_2\mathcal{Q}_2\mathcal{Q}_3^\#\right)^2}}\right)$$

$$\mathcal{Q}^\flat = \frac{\mathcal{Q}_1 + \mathcal{Q}_3^\flat + \ell_2\mathcal{Q}_1\mathcal{Q}_3^\flat}{2}\left(1 + \sqrt{1 + \frac{4(\ell_1 - 1)\mathcal{Q}_1\mathcal{Q}_3^\flat}{\left(\mathcal{Q}_1 + \mathcal{Q}_3^\flat + \ell_2\mathcal{Q}_1\mathcal{Q}_3^\flat\right)^2}}\right)$$

For the example illustrated in Fig. 3C we took $\lambda_1 = \lambda_4 = \beta_{11}I_1 + \beta_{11}(I_3 + I_4)/2$, $\lambda_2 = \lambda_3 = \beta_{22}I_2 + \beta_{11}(I_3 + I_4)/2$, and $\alpha_3 = \alpha_4 = \alpha_1 + \alpha_2$. Fig. 3C shows that as $\mathcal{R}^\#$ is increased, the stable steady state changes from one with PV2 only present to the state with both variants present. The bifurcation occurs when $\mathcal{Q}^\flat = 1$. As $\mathcal{R}^\#$ is increased further, the prevalence of PV2 becomes zero when $\mathcal{Q}^\# = 1$. The steady state with PV1 only is then present with $\mathcal{Q}^\# < 1$, but increasing $\mathcal{R}^\#$ further we obtain $\mathcal{Q}^\# > 1$ and the steady state with both variants is again present and stable.

Special Case 4. Two pathogen variants with no interaction.

With no interaction between PV1 and PV2 we have $\lambda_1 = \lambda_4 = \beta_{11}(I_1 + I_3 + I_4)$, $\lambda_2 = \lambda_3 = \beta_{22}(I_2 + I_3 + I_4)$, $\alpha_3 = \alpha_4$, $k_j = \ell_j = 1$ for $j = 1, 2, 3$, $\mathcal{Q}_3^\# = \mathcal{Q}_4^\#$, and $\mathcal{Q}_3^\flat = \mathcal{Q}_4^\flat$. The threshold quantities are

$$\mathcal{Q}^\# = \mathcal{Q}_2 + \mathcal{Q}_3^\# + \mathcal{Q}_2\mathcal{Q}_3^\#$$
$$\mathcal{Q}^\flat = \mathcal{Q}_1 + \mathcal{Q}_3^\flat + \mathcal{Q}_1\mathcal{Q}_3^\flat$$

This example is illustrated in Fig. 3D with $\alpha_3 = \alpha_4 = \alpha_1 + \alpha_2$. Fig. 3D shows that as $\mathcal{R}^\#$ is increased, the stable steady state changes from one with PV2 only present to the state with both variants present. The bifurcation occurs when $\mathcal{Q}^\flat = 1$.

Special Case 5. One pathogen variant enhances transmission of the other variant.

If infection with PV2 enhances the transmission of PV1, we need $\lambda_4 > \lambda_1$. If the ratios β_{14}/β_{44} and β_{13}/β_{43} are equal, then $\ell_3 = 1$ and Eqs. (6), (8) lead to

$$\mathcal{Q}^\# = \frac{\mathcal{Q}_2 + \mathcal{Q}_3^\# + k_2\mathcal{Q}_2\mathcal{Q}_4^\#}{2}\left(1 + \sqrt{1 + \frac{4\mathcal{Q}_2\mathcal{Q}_3^\#\left(k_1 - 1 + k_2(k_3 - 1)\mathcal{Q}_4^\#\right)}{\left(\mathcal{Q}_2 + \mathcal{Q}_3^\# + k_2\mathcal{Q}_2\mathcal{Q}_4^\#\right)^2}}\right)$$

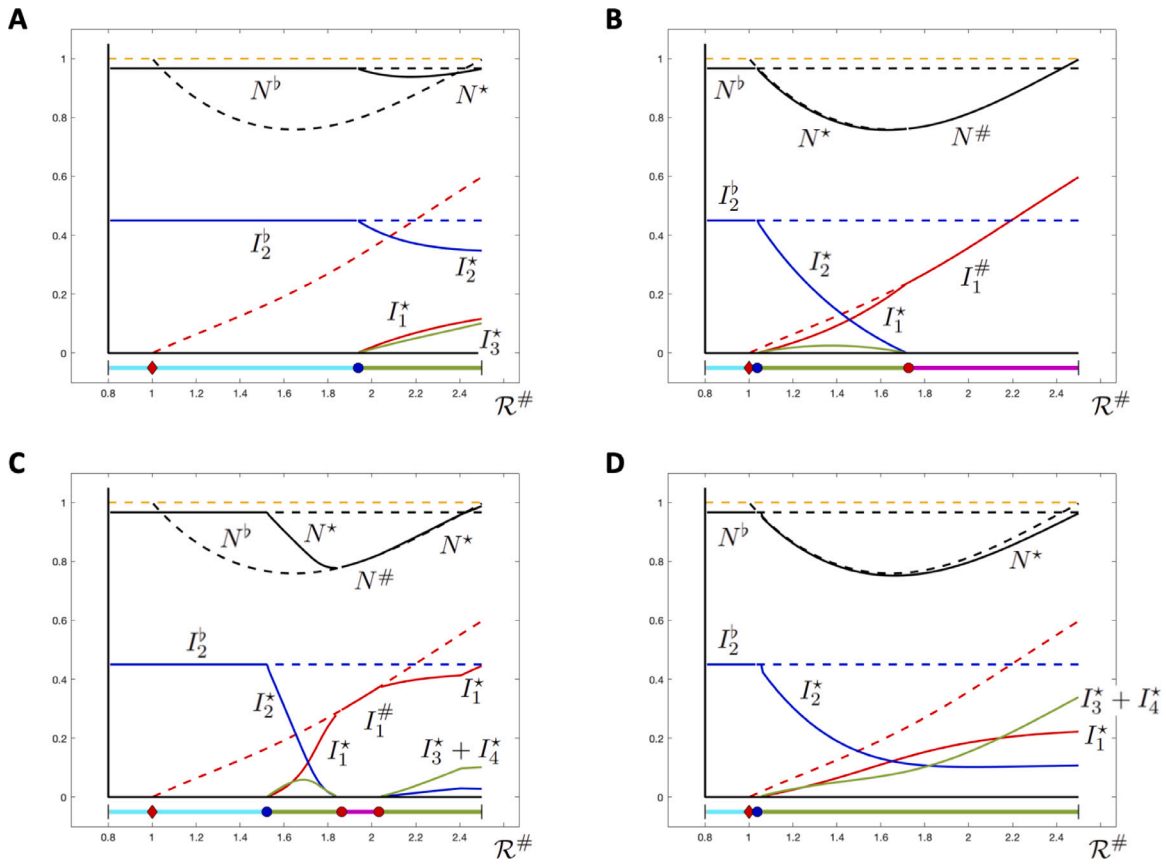

Fig. 3. Bifurcation diagrams against $\mathcal{R}^\#$ for A: Special Case 2 where infection with pathogen variant two (PV2) excludes pathogen variant one (PV1); B: Special Case 2 where infection with PV1 excludes PV2; C: Special Case 3 where the order of infection is immaterial; and D: Special Case 4 where PV1 and PV2 do not interact. Host population density is shown in black, density of hosts infected with PV1 only in red, density of hosts infected with PV2 only in blue, density of hosts infected with both variants in green, host carrying capacity in orange. Solid curves show a stable steady state, broken curves an unstable state. The lower bars indicates the stable steady state at that value of $\mathcal{R}^\#$. Cyan: $(N^\flat, 0, I_2^\flat)$; Green: $(N^\star, I_1^\star, I_2^\star)$. At the red diamonds $\mathcal{R}^\# = 1$, at the blue circles $\mathcal{Q}^\flat = 1$, and at the red circles $\mathcal{Q}^\# = 1$.

$$\mathcal{Q}^\flat = \frac{\mathcal{Q}_1 + \ell_2\mathcal{Q}_1\mathcal{Q}_3^\flat + \mathcal{Q}_4^\flat}{2}\left(1 + \sqrt{1 + \frac{4\left(\ell_1 - 1\right)\mathcal{Q}_1\mathcal{Q}_4^\flat}{\left(\mathcal{Q}_1 + \ell_2\mathcal{Q}_1\mathcal{Q}_3^\flat + \mathcal{Q}_4^\flat\right)^2}}\right)$$

This is the situation used in the first example illustrating this special case, see Table 1 and Fig. 4A. It can be seen in the figure that, in contrast to the previous examples, $\mathcal{Q}^\flat = 1$ at a value $\mathcal{R}^\# < 1$. This means that PV1 persists for some values of $\mathcal{R}^\# < 1$, due to enhanced transmission in the presence of PV2.

If infection with PV1 enhance the transmission of PV2, we require $\lambda_3 > \lambda_2$. If the ratios β_{23}/β_{33} and β_{24}/β_{34} are equal, then $k_3 = 1$ and Eqs. (6), (8) lead to

$$\mathcal{Q}^\# = \frac{\mathcal{Q}_2 + \mathcal{Q}_3^\# + k_2\mathcal{Q}_2\mathcal{Q}_4^\#}{2}\left(1 + \sqrt{1 + \frac{4\left(k_1 - 1\right)\mathcal{Q}_2\mathcal{Q}_3^\#}{\left(\mathcal{Q}_2 + \mathcal{Q}_3^\# + k_2\mathcal{Q}_2\mathcal{Q}_4^\#\right)^2}}\right)$$

$$\mathcal{Q}^\flat = \frac{\mathcal{Q}_1 + \ell_2\mathcal{Q}_1\mathcal{Q}_3^\flat + \mathcal{Q}_4^\flat}{2}\left(1 + \sqrt{1 + \frac{4\mathcal{Q}_1\mathcal{Q}_4^\flat\left(\ell_1 - 1 + \ell_2\left(\ell_3 - 1\right)\mathcal{Q}_3^\flat\right)}{\left(\mathcal{Q}_1 + \ell_2\mathcal{Q}_1\mathcal{Q}_3^\flat + \mathcal{Q}_4^\flat\right)^2}}\right)$$

Fig. 4B shows the variation of the coexistent steady state for this example, see the parameter values in Table 1. The figure shows that the steady state is stable over all parameter values exhibited.

3. Discussion

The usual route to determining invasion thresholds is via a local stability analysis based on eigenvalues of the Jacobian matrix [6,7,15]. The next-generation matrix (NGM) is usually used to determine if a pathogen can invade a fully susceptible host population [1,16]. Here we have used the concept to determine if one pathogen variant (species or strain) can invade and establish in a wild animal population where another pathogen variant is already endemic. In [3] the eigenvalues of a modified NGM were used to determine *invasion reproduction numbers* for an *SIS* model in a constant (human) population. As the modified NGM is two-dimensional the threshold may be found from a quadratic equation. In deriving expressions for the NGM, Eqs. (5), (7), we argued from epidemiological principles. In Appendix B we derive the NGM from the Jacobian matrix. Starting with the five-dimensional Jacobian we show that the ecological sub-matrix is stable, then apply the NGM formula to the three-dimensional epidemiological sub-matrix to evaluate the NGM of large domain [16]. The NGM formula requires specification of transmission and transition matrices. Consider, for example, a population infected with pathogen variant one (PV1) in a steady state. In evaluating the NGM for pathogen variant two (PV2), we observe that after a fully susceptible host has been infected with PV2, and is therefore in the I_2 compartment, subsequent infection with PV1 results in a transition from I_2 to I_4. Hence in Appendix B the term $\beta_{41}I_1^\#$ appears in the $\boldsymbol{\Sigma}^\#$ matrix, not in $\mathbf{T}^\#$.

In Fig. 2 we illustrate the special case where infection of an individual host with either pathogen excludes the other. Starting with the

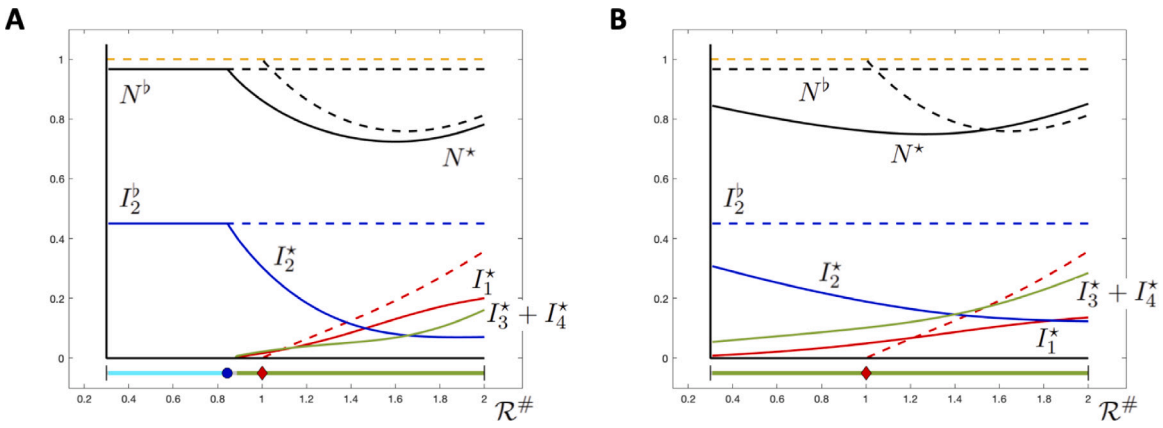

Fig. 4. Bifurcation diagrams against $\mathcal{R}^\#$ for Special Case 5. A: infection with pathogen variant two (PV2) enhances transmission of pathogen variant one (PV1); B: infection with PV1 enhances transmission of PV2. Host population density is shown in black, density of hosts infected with PV1 only in red, density of hosts infected with PV2 only in blue, density of hosts infected with both variants in green, host carrying capacity in orange. Solid curves show a stable steady state, broken curves an unstable state. The lower bars indicates the stable steady state at that value of $\mathcal{R}^\#$. Cyan: $\left(N^\flat, 0, I_2^\flat\right)$; Green: $\left(N^\star, I_1^\star, I_2^\star\right)$. At the red diamonds $\mathcal{R}^\# = 1$, at the blue circle $\mathcal{Q}^\flat = 1$.

population infected with PV2 in a steady state, we determine properties of PV1 that enable it to invade. We do this by decreasing the host mortality due to PV1, hence increasing its reproduction number $\mathcal{R}^\#$. If PV2 were not present in the population, PV1 could establish for $\mathcal{R}^\# > 1$, as shown by the broken curve in Fig. 2A. Changing values of $\mathcal{R}^\#$ changes the values of the threshold conditions $\mathcal{Q}^\#$ and $\mathcal{Q}^\flat$. For low values of $\mathcal{R}^\#$ we have $\mathcal{Q}^\# > 1$ and $\mathcal{Q}^\flat < 1$, hence PV1 cannot invade the steady state with PV2 only. At high values, $\mathcal{Q}^\# < 1$ and $\mathcal{Q}^\flat > 1$, hence PV1 is at steady state and PV2 cannot persist. There are intermediate values of $\mathcal{R}^\#$ where $\mathcal{Q}^\# > 1$ and $\mathcal{Q}^\flat > 1$, and both pathogens persist in the host population.

Similar bifurcation diagrams are shown in Fig. 3. For the special case where PV2 excludes PV1, it is unsurprising that the threshold $\mathcal{Q}^\flat = 1$, where PV1 can invade, is at a higher value of $\mathcal{R}^\#$ (Fig. 3A). In contrast, where PV1 excludes PV2 the threshold $\mathcal{Q}^\flat = 1$ is very close to $\mathcal{R}^\# = 1$, and PV2 is excluded from the population when $\mathcal{Q}^\# > 1$ (Fig. 3B). It must be emphasised that, for these two special cases, exclusion of one pathogen by another refers to within the same individual host, PV1 and PV2 may both persist within the host population if $\mathcal{Q}^\# > 1$ and $\mathcal{Q}^\flat > 1$. For the special case where the transition rates of hosts infected with both pathogens are independent of the order in which they were infected, we observe regions in parameter space where PV1 only, PV2 only, or both pathogens may persist. As $\mathcal{R}^\#$ is increased, the stable steady state changes from one with PV2 only to one with both pathogens present ($\mathcal{Q}^\# > 1$ and $\mathcal{Q}^\flat > 1$) to a state with PV1 only ($\mathcal{Q}^\# < 1$ and $\mathcal{Q}^\flat > 1$), then back to a steady state with both pathogens present (Fig. 3C). Where there is no direct interaction between the pathogens, the reason that the threshold $\mathcal{Q}^\flat = 1$ does not coincide with $\mathcal{R}^\# = 1$ is the increased host mortality due to infection with PV2 (Fig. 3D).

Bifurcation diagrams for the special cases where infection with one pathogen enhances transmission of the other are shown in Fig. 4. In both cases we have $\mathcal{Q}^\flat > 1$ for some values of $\mathcal{R}^\# < 1$. Where infection with PV2 increases susceptibility to PV1 the threshold $\mathcal{Q}^\flat = 1$ is at a value of $\mathcal{R}^\#$ just below one (Fig. 4A). Where infection with PV1 increases susceptibility to PV2 the effect is more pronounced, which seems at first counter-intuitive (Fig. 4B). However, the steady state with PV1 only present is unstable for $\mathcal{R}^\# > 1$ (broken curve) as PV2 is able to invade, the equilibrium state being that with both pathogens over the range of parameters displayed.

For all of the examples presented in Figs. 2–4 numerical simulations (not shown) confirmed that the stable steady states were unique. No instances of bistability or periodic behaviour were observed. The model presented is limited to directly transmitted endemic infections, and our primary focus was to derive threshold quantities for the invasion of a second pathogen. The assumption was that infection with one pathogen may influence the susceptibility or transmission of the other. Further work will examine the interaction of seasonal pathogens, and the interaction of vector transmitted pathogens.

CRediT authorship contribution statement

M.G. Roberts: Writing – review & editing, Writing – original draft, Project administration, Methodology, Funding acquisition, Formal analysis, Conceptualization.

Declaration of competing interest

The author declares no conflict of interest.

Acknowledgements

This research was supported by the Marsden Fund New Zealand under contract 20-MAU-50. Comments by two anonymous referees led to improvements in the manuscript.

Appendix A. Steady states with a single pathogen

From Eqs. (1), (2) the steady state with PV1 only present has infection prevalence

$$\frac{I_1^\#}{N^\#} = \frac{\nu(N^\#) - \mu(N^\#)}{\alpha_1} = 1 - \frac{\mu(N^\#) + \alpha_1}{\beta_{11} N^\#}$$

For a solution with $N^\# > I^\# > 0$ it is necessary that $\beta_{11} N^\# > \mu(N^\#) + \alpha_1$, so $N^\# > \alpha_1/\beta_{11}$. Combining the two expressions for $I_1^\#/N^\#$ above, $N^\#$ solves

$$F(N) = \left(\frac{\nu(N) - \mu(N)}{\alpha_1} - 1\right) N + \frac{\mu(N) + \alpha_1}{\beta_{11}} = 0$$

If $\widetilde{N} = \alpha_1/\beta_{11}$ then $F(\widetilde{N}) = \nu(\widetilde{N})/\beta_{11} > 0$. Also, if $\mathcal{R}^\# > 1$ then $\beta_{11} K > \mu(K) + \alpha_1$ and $F(K) = \left(\mu(K) + \alpha_1\right)/\beta_{11} - K < 0$. Hence there exists at least one solution $F(N^\#) = 0$, and the solution is bounded $\alpha_1/\beta_{11} < N^\# < K$. Differentiating and substituting leads to

$$F'(N^\#) = \left(\frac{I^\#}{N^\#} - 1\right) + \frac{\nu'(N^\#) N^\#}{\alpha_1} + \frac{\mu'(N^\#)}{\alpha_1}\left(\frac{\alpha_1}{\beta_{11}} - N^\#\right)$$

As $I^\# < N^\#$ the first term is negative. The other two terms are non-positive, hence $F'(N^\#) < 0$ and the solution $F(N^\#) = 0$ is unique. Similarly, the unique steady state with PV2 only present, exists when $\mathcal{R}^\flat > 1$ and is bounded $\alpha_2/\beta_{22} < N^\flat < K$.

Appendix B. The Jacobian and next-generation matrices

The Jacobian matrix of Eqs. (1)–(4) is

$$\mathbf{J}=\begin{pmatrix} \nu(N)-\mu(N)+\{\nu'(N)-\mu'(N)\}N & -\alpha_1 & -\alpha_2 & -\alpha_3 & -\alpha_4 \\ \lambda_1-\mu'(N)I_1 & \beta_{11}S-\lambda_1-\{\mu(N)+\alpha_1+\lambda_3\} & -\lambda_1-\beta_{32}I_1 & \beta_{13}S-\lambda_1-\beta_{33}I_1 & \beta_{14}S-\lambda_1-\beta_{34}I_1 \\ \lambda_2-\mu'(N)I_2 & -\lambda_2-\beta_{41}I_2 & \beta_{22}S-\lambda_2-\{\mu(N)+\alpha_2+\lambda_4\} & \beta_{23}S-\lambda_2-\beta_{43}I_2 & \beta_{24}S-\lambda_2-\beta_{44}I_2 \\ -\mu'(N)I_3 & \lambda_3 & \beta_{32}I_1 & \beta_{33}I_1-\{\mu(N)+\alpha_3\} & \beta_{34}I_1 \\ -\mu'(N)I_4 & \beta_{41}I_2 & \lambda_4 & \beta_{43}I_2 & \beta_{44}I_2-\{\mu(N)+\alpha_4\} \end{pmatrix}$$

At the steady state with PV1 only present, the matrix is structured

$$\mathbf{J}=\begin{pmatrix} J_{11} & -\alpha_1 & -\alpha_2 & -\alpha_3 & -\alpha_4 \\ J_{21} & -\beta_{11}I_1^{\#} & J_{23} & J_{24} & J_{25} \\ 0 & 0 & J_{33} & J_{34} & J_{35} \\ 0 & 0 & \beta_{32}I_1^{\#} & J_{44} & \beta_{34}I_1^{\#} \\ 0 & 0 & \beta_{41}I_1^{\#} & 0 & J_{55} \end{pmatrix}$$

and the eigenvalues of $\mathbf{J}$ are independent of J_{23}, J_{24} and J_{25}. Two eigenvalues of $\mathbf{J}$ are the roots of the quadratic equation

$$\lambda^2-\left(J_{11}+J_{22}\right)\lambda+\left(J_{11}J_{22}-J_{12}J_{21}\right)=0$$

We have

$$J_{11}+J_{22}=\left(\alpha_1-\beta_{11}N^{\#}\right)\frac{I_1^{\#}}{N^{\#}}+\left\{\nu'(N^{\#})-\mu'(N^{\#})\right\}N^{\#}$$

$$J_{11}J_{22}-J_{12}J_{21}=\alpha_1\beta_{11}\left(1-\frac{I_1^{\#}}{N^{\#}}-\frac{\nu'(N^{\#})N^{\#}}{\alpha_1}\right)I_1^{\#}+\mu'(N^{\#})\left(\beta_{11}N^{\#}-\alpha_1\right)I_1^{\#}$$

As $\nu'(N)\leqslant 0$, $\mu'(N)\geqslant 0$, $\beta_{11}N^{\#}>\alpha_1$ and $I_1^{\#}<N^{\#}$ we have $J_{11}+J_{22}<0$ and $J_{11}J_{22}-J_{12}J_{21}>0$. Hence the quadratic equation is stable. The other three eigenvalues of $\mathbf{J}$ are the eigenvalues of the epidemiological stability matrix (ESM) $\mathbf{H}^{\#}=\mathbf{T}^{\#}+\mathbf{\Sigma}^{\#}$, where the transmission matrix is

$$\mathbf{T}^{\#}=\begin{pmatrix} \beta_{22}\left(N^{\#}-I_1^{\#}\right) & \beta_{23}\left(N^{\#}-I_1^{\#}\right) & \beta_{24}\left(N^{\#}-I_1^{\#}\right) \\ \beta_{32}I_1^{\#} & \beta_{33}I_1^{\#} & \beta_{34}I_1^{\#} \\ 0 & 0 & 0 \end{pmatrix}$$

and the transition matrix is

$$\mathbf{\Sigma}^{\#}=\begin{pmatrix} -\left\{\mu(N^{\#})+\alpha_2+\beta_{41}I_1^{\#}\right\} & 0 & 0 \\ 0 & -\left\{\mu(N^{\#})+\alpha_3\right\} & 0 \\ \beta_{41}I_1^{\#} & 0 & -\left\{\mu(N^{\#})+\alpha_4\right\} \end{pmatrix}$$

Applying the NGM formula [16] to the ESM, the NGM of large domain is $\mathbf{K}_L^{\#}=-\mathbf{T}^{\#}\mathbf{\Sigma}^{\#-1}$, and

$$\mathbf{K}_L^{\#}=\begin{pmatrix} \dfrac{\beta_{22}\left(N^{\#}-I_1^{\#}\right)}{\mu(N^{\#})+\alpha_2+\beta_{41}I_1^{\#}}+\dfrac{\beta_{24}\beta_{41}\left(N^{\#}-I_1^{\#}\right)I_1^{\#}}{\left(\mu(N^{\#})+\alpha_2+\beta_{41}I_1^{\#}\right)\left(\mu(N^{\#})+\alpha_4\right)} & \dfrac{\beta_{23}\left(N^{\#}-I_1^{\#}\right)}{\mu(N^{\#})+\alpha_3} & \dfrac{\beta_{24}\left(N^{\#}-I_1^{\#}\right)}{\mu(N^{\#})+\alpha_4} \\ \dfrac{\beta_{32}I_1^{\#}}{\mu(N^{\#})+\alpha_2+\beta_{41}I_1^{\#}}+\dfrac{\beta_{34}\beta_{41}I_1^{\#2}}{\left(\mu(N^{\#})+\alpha_2+\beta_{41}I_1^{\#}\right)\left(\mu(N^{\#})+\alpha_4\right)} & \dfrac{\beta_{33}I_1^{\#}}{\mu(N^{\#})+\alpha_3} & \dfrac{\beta_{34}I_1^{\#}}{\mu(N^{\#})+\alpha_4} \\ 0 & 0 & 0 \end{pmatrix}$$

The NGM, $\mathbf{K}^{\#}$, is then the leading 2×2 sub-matrix of $\mathbf{K}_L^{\#}$, see Eq. (5). Pathogen variant two can invade if $\rho(\mathbf{K}^{\#})>1$. Similarly, the steady state with PV2 only present can be invaded by PV1 if $\rho(\mathbf{K}^{b})>1$, see Eq. (7).

References

[1] O. Diekmann, JAP. Heesterbeek, Mathematical Epidemiology of Infectious Diseases: Model Building, Analysis and Interpretation, Wiley, Chichester, 2000.

[2] O. Diekmann, J.A.P. Heesterbeek, T. Britton, Mathematical Tools for Understanding Infectious Disease Dynamics, Princeton University Press, Princeton, 2013.

[3] D. Gao, T.C. Porco, S. Ruane, Coinfection dynamics of two diseases in a single host population, J. Math. Anal. Appl. 442 (2016) 171–188.

[4] L.-I.W. Roeger, Z. Feng, C. Castillo-Chavez, Modeling TB and HIV co-infections, Math. Biosci. Eng. 6 (2009) 815–837.

[5] S.W. Teklu, Y.F. Abebaw, B.B. Terefe, D.K. Mamo, HIV/AIDS and TB co-infection deterministic model bifurcation and optimal control analysis, Inform. Med. Unlocked 41 (2023) 101328.

[6] C.-L. Wang, S. Gao, X.-Z. Li, M. Martcheva, Modeling syphilis and HIV coinfection: A case study in the USA, Bull. Math. Biol. 85 (2023) 20.

[7] Z. Mukandavire, A.B. Gumel, W. Garira, J.M. Tchuenche, Mathematical analysis of a model for HIV-malaria co-infection, Math. Biosci. Eng. 6 (2009) 333–362.

[8] K.G. Mekonen, L.L. Obsu, Mathematical modeling and analysis for the co-infection of COVID-19 and tuberculosis, Heliyon 8 (2022) e11195.

[9] D. Salkeld, S. Hopkins, D. Hayman, Emerging Zoonotic and Wildlife Pathogens, Oxford University Press, 2023.

[10] M.G. Roberts, A.P. Dobson, The population dynamics of communities of parasitic helminths, Math. Biosci. 126 (1995) 191–214.

[11] A. Dimas Martins, Q. ten Bosch, JAP. Heesterbeek, Exploring the influence of competition on arbovirus invasion risk in communities, PLoS ONE 17 (2022) e0275687.

[12] D.M. Tufts, B. Adams, M.A. Diuk-Wasser, Ecological interactions driving population dynamics of two tick-borne pathogens, *Borrelia burgdorferi* and *Babesia microti*, Proc. R. Soc. Ser. B 290 (2023) 20230642.

[13] M.Z. Ndii, R.I. Hickson, D. Allingham, G.N. Mercer, Modelling the transmission dynamics of dengue in the presence of wolbachia, Math. Biosci. 262 (2015) 157–166.

[14] A.J. Kucharski, V. Andreasen, J.R. Gog, Capturing the dynamics of pathogens with many strains, J. Math. Biol. 72 (2016) 1–24.

[15] M.A. Kuddus, E.S. McBryde, A.I. Adekunl, L.J. White, M.T. Meehan, Mathematical analysis of a two-strain disease model with amplification, Chaos Solitons Fractals 143 (2021) 110594.

[16] O. Diekmann, J.A.P. Heesterbeek, M.G. Roberts, The construction of next-generation matrices for compartmental epidemic models, J. R. Soc. Interface 7 (2010) 873–885.